APPENDIX II.5

LINEAR RHEOLOGY OF POLYDISPERSE LINEAR AND STAR-SHAPED POLY-(METHYL METHACRYLATE)

This chapter presents some results obtained on linear and star PMMA samples. They will be used to write an article in collaboration with JF. Vega and L. Xue (Eindhoven).

5.1 INTRODUCTION

Understanding and predicting viscoelastic response of polymer melts from the knowledge of their molecular structure is an enduring issue in polymer science[1,2,3,4]. It has important ramifications for very practical as well as fundamental questions. Indeed, satisfactory physical models can be used to help predict processing performance as well as to clarify molecular dynamics in the melt.

In the last two decades, while predictions of linear viscoelasticity have reached a quantitative level of accuracy for linear polymer melts, the situation is less satisfactory for branched molecules, despite the many efforts which have been undertaken. Branched polymers exhibit a behaviour quite different from the behaviour of linear polymers. Indeed, it is assumed that a linear chain relaxes by reptation,[1,2] i.e. by translation in a curvilinear fashion along its own contour length in a tube shaped by the surrounding molecules.[2] If the polymer molecule is branched, this simple chain snake-like motion will be strongly impeded, resulting in a different relaxation mechanism, and as a consequence in a distinct rheological behaviour. It is considered that these molecules mainly relax by free arm retraction and subsequent exploration of the new tube[5]. Tube length fluctuations lead to an

exponential dependence of relaxation times (or viscosities) on the number of entanglements per branch, which it is actually experimentally observed, and to the constraint release mechanism known as dynamic dilution[6,7]. Mostly because fluctuations are very dependent on the details of the molecular architecture, understanding and predicting the viscoelastic behaviour of an industrial branched polymer represents a complex issue. For this reason, star polymers, which are the simplest branched molecules, play an important role as model systems and are a good starting point towards quantitative predictions of more complex polymers.

Different models have been proposed to predict the linear viscoelasticity (LVE) of monodisperse symmetric stars[3,8,9], blends of two monodisperse symmetric stars[10], or monodisperse asymmetric stars[11]. Nevertheless, these models do not allow predictions of LVE for polydisperse linear or star polymers.
Recently we have modified existing tube models in order to describe the linear viscoelastic behaviour of polydisperse blends of linear and star molecules.[12] The main feature of this model is that there is no time scale separation between reptation and fluctuations processes. Indeed, the model is based on a time marching algorithm, calculating the relaxation function *G(t)* step by step through time and treating reptation and fluctuations as simultaneous and progressive processes. The polymer fraction already relaxed and acting as solvent for the relaxation of the remaining oriented part of the polymer is continuously taken into account in the relaxation of the polymer melt. So, no limitation concerning polydispersity is imposed, which is essential to treat polydisperse star polymers.

The aim of this work is to test our model on 6-arm star-shaped polydisperse star PMMA samples synthesized by L. Xue at the University of Eindhoven[13]. The synthesis of the star polymers is briefly described in Section 5.2.A.The rheological behaviour of the star-shaped samples and of linear reference samples has been measured by J.F. Vega at the University of Eindhoven[14] over a wide range of molecular weights and temperatures. The experimental procedures are described in Section 5.2.B. Although a few

publications exist, concerning the viscoelastic behaviour of linear PMMA, as far as we know, there are no data in literature concerning star-shaped PMMA. The material parameters needed to calibrate our model have been extracted from the data by J.F. Vega[14]. The procedure followed and the results are described in Section 5.3.A. We use these material parameters (with some modifications) to test the predictions of our model in Section 5.3.B

5.2 EXPERIMENTAL SECTION

5.2.1 Materials and molecular characterization

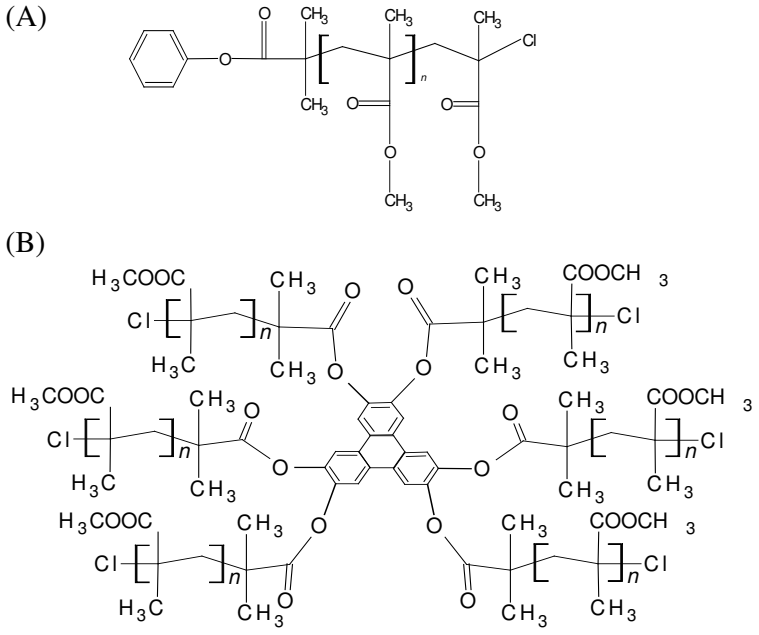

Figure 1. Chemical structures of the linear PMMA (A) and the six-arm star PMMA (B), synthesized as described in references 13 and 15.

The linear and six-arm star PMMA samples were synthesized by atom transfer radical polymerization (ATRP), with CuCl as catalyst combined with 4,4'-di-*n*-nonyl-2,2'-bipyridine (d*n*Nbpy).[13,15] The linear PMMA samples were initiated from a monofunctional initiator, phenyl 2-bromo-2-methylpropionate (BMPE). The well-defined 6-arm star PMMA samples were initiated from a hexafunctional initiator, 2,3,6,7,10,11-triphenylene-hexa-2-bromo-2-methylpropionate TP6Br. Figure 1 shows their chemical structures.

A detailed description of the molecular and structural characterization techniques used for the materials is available elsewhere.[15] Molecular and structural parameters are listed in Table I.

Table I. Molecular and structural parameters of linear and star PMMA

Material	M_w g mol^{-1}	M_w/M_n	Triad ratio mm:rm:rr)[a]	T_g ºC
0093-1 (L30)	33000	1.11	12:34:54	104.4
121F (L70)	76100	1.13	6:35:59	122.2
122F (L90)	90400	1.23	6:35:59	123.6
146B (L200)	213500	1.29	12:31:57	101.0
0161-02 (S190)	130500	1.26	4:35:61	114.5
0161-1 (S260)	210600	1.24	6:35:59	119.9
0144-10 (S500)	535000	1.20	5:35:59	127.7
230403-07 (S1200)	1200000	1.20	3:29:68	131.0
240403-01 (S2500)	2500000	1.30	4:36:60	125.0

a) mm, rm and rr represent the isotactic, heterotactic and syndiotactic methyl protons (-CH_3).

5.2.2 Rheological measurements

Dynamic moduli were obtained on the samples with an Advanced Rheometrics Expanded Spectrometer (ARES) in the parallel plates mode. The storage modulus, G', and loss modulus, G'', were obtained as functions of angular frequency ω in the frequency range 0.001 radians/s to 100 radians/s. Two different geometries with radii 4 mm and 12.5 mm, depending on the temperature (moduli), were used. The gap between the plates was set between 0.5 and 1.0 mm. The measurements were performed in the linear viscoelastic regime located by previous strain sweeps. Linearity was confirmed repeatedly by measurements at different strain values, typically between 0.001-0.1. Prior to frequency sweep it was necessary a distinct heating and measure procedures to obtain reproducible measurements, due to an adhesion kinetics of the samples to the plates. We have followed a similar procedure than Fuchs and co-workers (1996).

The PMMA powders were mixed with 0.5% Irganox and molded in a hot-press at 160 ºC into clear, bubble-free disks. Measurements were made between 130 and 220 ºC. The thermo stated oven was flushed continuously with high-purity nitrogen. Repeat measurements at low frequencies were used to check for sample degradation.

Master curves were obtained from measurements at different temperatures and superimposed to the data at a reference temperature of T_0=190ºC by experimental shift factors (a_T) along the frequency axis. Small vertical shifts (b_T) have been required in the temperature range used. Within the temperature range explored, the time-temperature superposition has been found to be applicable in all the samples, and the shift factors a_T obey the Williams-Landel-Ferry (WLF) equation:[16]

$$\log a_T = \frac{c_1^{\,0}(T - T_0)}{c_2^{\,0} + (T - T_0)}. \qquad (1)$$

Averages values of $c_1^{\,0}$=6.0 and $c_2^{\,0}$=140ºC were obtained. To compare the values of $c_1^{\,0}$ and $c_2^{\,0}$ with those in the literature it is necessary to

use comparable reference temperatures. Usually the glass transition temperature, T_g, or the arbitrary temperature $T_s=T_g+50$, have been used. Considering an average value of $T_g=125ºC$ in our samples the values obtained are $c_1^s=11.2$ and $c_2^s=75$. Similar values can be found in the literature for a several number of polymer species[16].

Thermorheological simplicity of the branched samples has been verified. This is the norm in linear polymers, but a breakdown of TTS is often found in long chain branched flexible polymers as PE[17], HPBd, PBd, HPI[18], and PI[19]. This is not the case of star branched PMMA samples studied here, as in other big side group polymers like star PS and PIB.

5.3 RESULTS AND DISCUSSION

5.3.1 Material parameters

In addition to the zero shear viscosity and the compliance, the usual material parameters to describe the linear viscoelasticity of a well-entangled polymer melt are the plateau modulus, G_N^0, the molecular weight between two entanglements, M_e, and the Rouse relaxation time τ_e of a chain segment between two entanglements. Because these three parameters allow to completely define the proposed tube model, we determine them from the measured rheological data (storage and loss moduli, G'(ω) and G"(ω)).

Plateau modulus

Because of the storage modulus at intermediate frequencies does not become truly constant, the "plateau" modulus was estimated by applying the loss tangent minimum criterion, i.e. taking G_N^0 equal to the storage modulus, G', at the frequency where $tan\ \delta=G''/G'$ has its minimum in the "plateau" zone for the materials with the highest

molecular weight in order to eliminate contributions of the transition zone[20]:

$$G_N^0 = G'|_{\tan\delta \to \min}. \qquad (2)$$

The values of G_N^0 obtained are given in Table II. Long chain branching seems to have no influence on the melt entanglement state for high molecular weight. The data in Table II show that only small differences exist between the values of G_N^0 for linear and star branched polymers.

Table II. Rheological parameters of linear and star PMMA at T=190ºC

Material	G_N^0 (Pa)	M_e (g mol^{-1})	η_0 (Pa s)	J_e^0(Pa^{-1})
0093-1 (L30)	-	-	4600	$8.7\ 10^{-6}$
121F (L70)	-	-	63800	$9.6\ 10^{-6}$
122F (L90)	420000	8430	180000	$1.0\ 10^{-5}$
146B (L200)	430000	8240	900000	$2.1\ 10^{-5}$
0161-0 (S200)	-	-	27600	$3.3\ 10^{-5}$
0161-1 (S260)	-	-	97900	$5.6\ 10^{-5}$
0144-10 (S500)	470000	7535	$6.7\ 10^6$	$1.1\ 10^{-4}$-
230403-07 (S1200)	450000	7870	$>1\ 10^9$	-
240403-01 (S2500)	450000	7870	>1.0 10^{12}	-

Molecular weight between entanglements

From the plateau modulus, it is possible to estimate the entanglement molecular weight as:

$$M_e = K\frac{\rho RT}{G_N^0}, \qquad (3)$$

where ρ (1.15 g cm^{-3} at T=190ºC) is the density, R is the universal gas constant, T the absolute temperature and K a constant equal to 1 or 4/5 depending on the convention.[4,20] Average values of M_e=9600 and 7700 g mol^{-1} are obtained for K=1 and K=4/5, respectively. Comparisons with other data available for PMMA are possible. The values of M_e (and G_N^0) are strongly dependent on tacticity, ranging from M_e=17000 for pure isotactic PMMA to M_e=7700 for pure syndiotactic PMMA.[22] The values obtained here agree well with the ones corresponding to syndiotactic-rich PMMA.[21,22]

Rouse relaxation time of a segment

At this point, all the material parameters are known, except τ_e, the relaxation time (Rouse time) of an entanglement strand of molecular weight M_e. This characteristic relaxation time can be calculated from[2]:

$$\tau_e = \frac{z_0 \frac{\langle R^2 \rangle}{M} M_e^{\,2}}{3p^2 K_B T} m_0 \quad , \qquad (4)$$

where ζ_0 is the monomeric friction coefficient, $\langle R^2 \rangle / M$ is the monodisperse chain end-to-end distance molecular weight ratio for an ideal equilibrium random coil, M_e the average molecular weight between topological constraints, m_0 the molecular weight of the monomeric unit, K_B the Boltzmann constant, and T is the absolute temperature. We have collected the parameters involved in Equation 4 (see Table III) from the literature for linear and star (symmetric) branched PS,[23] PBd,[24,25] PIB[26,27] and PMMA.[16,28,29]

Table III. Parameters used for the calculation of τ_e for the comparison of η_0 (Figure 2) for linear and star-shaped polymers.

Material	ζ_0[42] N m s^{-1}	$\langle R^2 \rangle / M$[48,49] $Å^2 g^{-1} mol$	M_e[48,49] g mol^{-1}	T °K	m_0 g mol^{-1}	τ_e s
PBd	$1.4\ 10^{-10}$	0.876	1900	301	54	$6.03\ 10^{-7}$
PIB	$4.5\ 10^{-8}$	0.570	5500	298	56	$1.14\ 10^{-3}$
PMMA	*$1.1\ 10^{-6}$*	*0.500*	*7700*	*463*	*100*	*$1.8\ 10^{-3}$*
PS	$1.0\ 10^{-7}$	0.434	13500	433	104	$4.31\ 10^{-3}$

In order to validate the Rouse relaxation time calculated from these parameters, we have used chemistry independent variables by plotting $\eta_0 G_N^0 / \tau_e$ *versus* N_e , and compared results obtained for PMMA samples with literature data for other polymers.

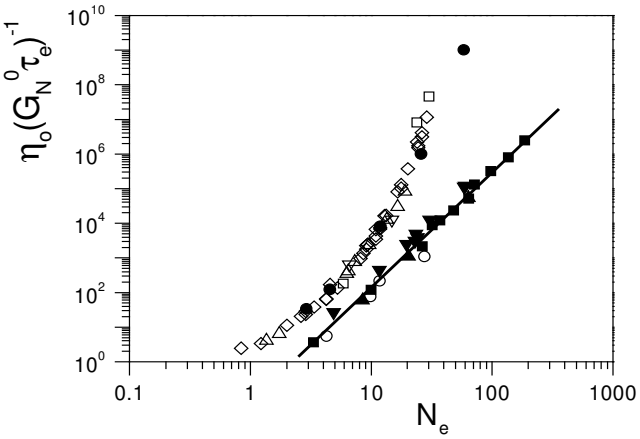

Figure 2. Comparison of the η_0 experimental values of linear and star polymers in normalized form $\eta_0 / G_N^0 \tau_e$ versus the number of entanglements per chain (linear samples) and per arm (star samples). (■) linear PBd[24], (□) star PBD, (◇) star PI[27], (▼) linear PIB, (▽) star PIB[26] (▲) linear PS, (△) star PS, (○) linear PMMA, and (●) star PMMA.

The values of η_0 of all samples, were obtained as:[16]

$$\eta_0 = \lim_{\omega \to 0} \frac{G''(\omega)}{\omega}. \qquad (5)$$

These data, reduced to 190 ºC, are collected in Table II. The result obtained can be seen in Figure 2.

All the data seem to collapse on unique master curves independent on the local chemistry, at least in this limited molecular weight range, as predicted by universal topological theories based on reptation and tube concepts.[1,2] However, in the case of PMMA, the ζ_0 value we have found in the literature is unable to explain the experimental results obtained,[16] so we have used our experimental η_0 and G_N^0 values to estimate the characteristic ζ_0 (or τ_e) value, included in Table III, by shifting the values of the reduced Newtonian viscosity to the master curves in Figure 2.

5.3.2 Comparison between experiments and theory

Starting from these material parameters, we can now use our model for predicting the storage and loss moduli of the linear and star PMMA samples, and compare the predictions with the experimental data.

Theory [12]

In this model, the relaxation function $G(t_k)$ of the polymer melt, which is proportional to the unrelaxed part of the polymer melt, is calculated from the weighted sum of the survival probabilities of all the segment of all the arms, at the observed time t_k. (A segment is defined by the normalized variable x_i, taking values between 0 and the end of the arm to 1 near its branching point):

$$G(t_k) = G_N^0 \cdot \left[\sum_i \varphi_i \int_0^1 \left(p_{rept}(x_i, t_k) \cdot p_{fluc}(x_i, t_k) \cdot p_{envir}(x_i, t_k) \right) dx_i \right], \quad (6)$$

where the parameter φ_i represents the volumetric fraction associated to the arm "*i*", and $p(x_i,t_k)$ represents the survival probability of the segment x_i on the arm *"i"*, at time t_k. Each segment can be relaxed in three different ways, which are explained below: reptation, fluctuations, or constraint release. Linear chains are considered as 2-arm stars.

The survival probabilities in $G(t_k)$ are upgraded at each time step. This allows to determine the corresponding polymer fraction, $\phi(t_k)$, not relaxed by reptation or fluctuations, which will act as a solvent for the relaxation of the remaining oriented part of the polymer. This "polymer solvent", which represents the constraint release mechanism, has also an influence on the reptation and fluctuations times of the segments[30].

The first term in Equation 6, $p_{rept}(x_i,t_k)$, determines the probability that the chain segment x_i is not relaxed by reptation. Its expression is based on the Doi & Edwards theory[2] and takes into account the past of the polymer (during which the reptation occurred according to another characteristic relaxation time τ_{rept}[12]):

$$p_{rept}(x_i, \Delta t) = \sum_{i\ odd} \frac{4}{p\pi} \sin\left(\frac{i\pi x_i}{2}\right) \exp\left(\frac{-i^2 (t_k - t_{k-1})}{\tau_{rept}(M)}\right), \quad (7)$$

$$p_{rept}(x_i, t_k) = p_{rept}(x_i, t_{k-1}) \cdot p_{rept}(x_i, \Delta t), \quad (8)$$

where $p_{rept}(x_i,\Delta t_k)$ represents the probability that the segment x_i is not relaxed by reptation between times t_k and t_{k-1}, and $\tau_{rept}(M,t_k)$ is the reptation time of the observed molecule, at time t_k:

$$\tau_{rept}(M) = 3\ \tau_e \left(\frac{M}{M_e} \right)^3 .\phi_{active}(t_k)^{\alpha}, \qquad (9)$$

where α is the dilution exponent[31,32,33] and $\phi_{active}(t_k)$ is generally equal to $\phi(t_k)$, the polymer fraction not relaxed by reptation or fluctuation at time t_k. Nevertheless, to have an active role in Equation 9, the time at which the polymer solvent has appeared and the observed time t_k must be well time-separated from the relaxation step under consideration[12,34,35].

The second term in Equation 6, $p_{fluc}(x_i,t_k)$, determines the probability that the segment x_i is not yet relaxed by tube length fluctuations at time t_k. The fluctuations time of a segment increases exponentially with its potential $U(x_i)$ resulting from the balance of the arm entropic spring force and of the tube constraint[31,61]:

$$\frac{\partial \ln \tau_a(x_i,t_k)}{\partial x_i} = \frac{\partial \left(U(x_i,t_k)/kT\right)}{\partial x_i} = 3 \cdot \left(\frac{M_i}{M_{e0}} \right) \cdot x_i \cdot \phi_{active}(t_k,x_i)^{\alpha}, \qquad (10)$$

As for the reptation process, the value of $\phi_{active}(x_i, t_k)$ depends on the time scales separation between the fluctuations time of the test molecule and the relaxation times of its environment.
Nevertheless, this fluctuation process does not describe the relaxation of the external arm segments, for which the potential is too small ($U<kT$) to be felt by the arm. Therefore, these segments fluctuate according an unconstrained Rouse process[5,12]:

$$\tau_{early}(x_i,t_k) = \frac{9\pi^3}{16} \cdot \left(\frac{M_a \cdot \phi_{rept}^{\alpha}(t_k)}{M_{e,0}} \right)^2 \cdot \tau_{R,chain} \cdot {x_i}^4, \qquad (11)$$

where $\tau_{R,chain}$ is the Rouse time of the entire arm and $\phi_{rept}(t)$ represents the polymer fraction not relaxed after the reptation process[12]. The transition between both mechanisms occurs at a segment called $x_{trans,i}$, for which the value of the potential is equal to kT:

$$\tau_{fluc}(x_i,t_k)=\tau_{early}(x_i,t_k) \qquad for\ \ x_i < x_{trans,i}\,, \quad (12)$$

$$\tau_{fluc}(x_i,t_k)=\tau_{early}(x_i,t_k)\exp\left(\frac{\Delta U(x_{trans,i}\rightarrow x_i,t_k)}{kT}\right), for\ \ x_i > x_{trans,i}\ . \quad (13)$$

From its fluctuations time, the survival probability of each segment after fluctuations is determined, in a way similar to the reptation process:

$$p_{fluc}(x_i,\Delta t)=\exp\frac{-(t_k-t_{k-1})}{\tau_{fluc}(x_i,t_k)}\,, \quad (14)$$

$$p_{fluc}(x_i,t_k)=p_{fluc}(x_i,t_{k-1})\cdot p_{fluc}(x_i,\Delta t)\,. \quad (15)$$

The last term of *G(t)* in Equation 6 describes the survival probability of a non relaxed segment (after reptation or fluctuation) if we consider the influence of the relaxation of its environment on its own relaxation. This is a constraint release mechanism, which is a generalization of double reptation ideas[36,37] to polymers that can be branched. Because the probability to loose an entanglement by constraint release is equivalent for all the segments in the polymer melt, this mechanism acts similarly on all the molecules, and can be represented by the dilation of the tube around the chains. The environment survival probability is equal to the probability that an entanglement taken at random in the polymer is still oriented, if we know that the observed segment x_i is not relaxed by reptation or by fluctuations. This additional condition informs us about the fact that all the segments requiring a fluctuations potential higher than the potential of x_i are also unrelaxed by fluctuation. Therefore, the general expression of the environment survival probability can be described by the following equation:

$$p_{envir}(x_i,t)=\left(\sum_k \varphi_k \cdot \left[\int_0^{x_{k,trans}} p_{rept}(x_k,t)\ p_{fluc}(x_k,t)\ dx_k + \int_{x_{k,trans}}^{1} p_{rept}(x_k,t)\ dx_k\right]\right)^{\alpha} \quad (16)$$

, where x_k represents the transition segment of arm k , equivalent (potential-wise) to the segment x_i.

So, the three terms in the relaxation function *G(t)* (Equation 6) are defined. This function is transformed into the storage and loss moduli *G'* and *G"* by using the Schwarzl functions[38].

Polydisperse linear samples

Staring from the experimental values of the material parameters G_N^0, M_e and τ_e, we have tried to predict the linear viscoelastic properties of the polydisperse linear PMMA samples. As expected, the plateau modulus is taken equal to 450000 Pa. But in this case, in order to have a good agreement between theory and experiments, the value of M_e must be equal to 9500 g/mol, which is a little higher than the expected 7800 g/mol. Nevertheless, this value stays in good agreement with experimental results obtained for syndiotactic-rich PMMA[21,22]. In order to keep the invariability of the plot of $(\eta_0/G_N^0\,\tau_e)$ versus the number of segments between entanglements N_e, the value of τ_e has been modified by a factor 9500/7800. Its value is thus equal to 2.3 10^{-3} s.

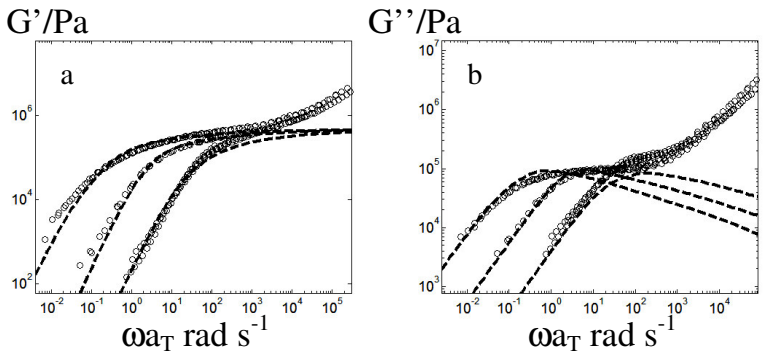

Figure 3. Master curves of the storage moduli G' (a) and loss moduli G" (b) (open symbols) of the linear PMMA samples at a reference temperature 190ºC. (from right to left:) L30, L70, L200. The dashed lines correspond to the calculated values of G' and G" in the terminal region.

The dilution exponent α has been fixed to 4/3, which is consistent with literature. Results are shown in Figure 3. The Rouse relaxation, which is useful to describe the behaviour of the polymer melt at high frequencies, is not taken into account in the predictions.

Polydisperse star samples

Next, these parameters, which have been determined to fit the linear samples, have been used to compare predictions and experiments of the polydisperse star PMMA (see Table I). Thus, in this case, we do not have any degree of freedom. Our predictions have been calculated from the molecular weight distribution of the cleaved arms for each sample[13]. The results for samples S190, S260 and S2500 are shown in Figure 4. They are in very good agreement with experiments. As already explained, the polydispersity of the sample is too high (near 1.2) to be neglected. Figure 5 illustrates this fact by showing the theoretical results obtained for sample S2500, using the same parameters as before but considering it as a monodisperse sample (with the same average M_w).

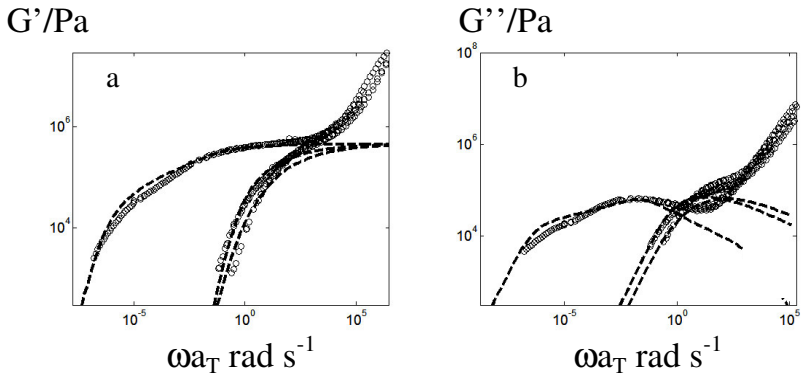

Figure 4. Master curves of the storage moduli, G' (a) and loss moduli, G" (b) (open symbols), of star branched PMMA samples at a reference temperature 190ºC: (from right to left:) S200, S260, S2500. The dashed lines correspond to the calculated values of G' and G" in the terminal region.

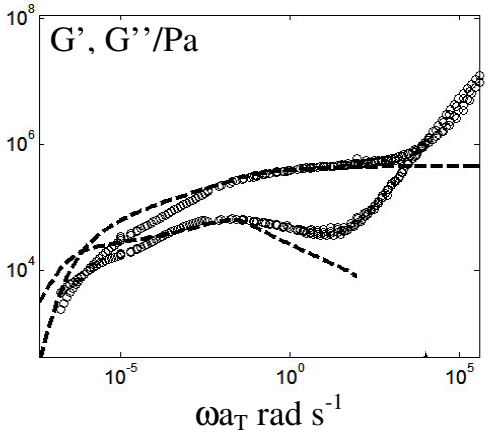

Figure 5. Master curves of the storage moduli, G' and loss moduli, G" (open symbols), of star branched PMMA sample S2500 at a reference temperature 190ºC. The dashed lines correspond to the calculated values of G' and G" in the terminal region, using a monodisperse distribution.

At low frequencies, predictions are very different from the ones obtained by considering the entire MWD and do not match the experimental data well.

Results obtained for sample S500 are presented in Figure 6.a.. As opposed to what is observed for the other star PMMA samples, our model theory predicts too quick a relaxation, in comparison with the experimental data.

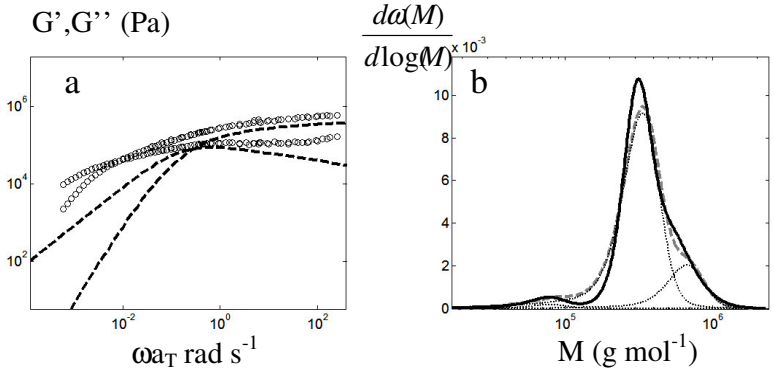

Figure 6. (a:) Master curves of the storage moduli, G' and loss moduli, G" (open symbols), of star branched PMMA sample S500 at a reference temperature 190ºC. The dashed lines correspond to the calculated values of G' and G" in the terminal region. (b:) (continuous line:) Molecular weight distribution of sample S500. (dashed line:) MWD rebuild from the MWD of cleaved arms (see text).

Even though this problem is not completely elucidated, we believe that it can be explained by the presence of more complex structures, like pom-pom molecules from star-star coupling, during polymerization. For this sample, as shown in Figure 6.b., we can indeed observe a shoulder on its MWD, which is not symmetric, contrary to the other samples[13]. This shoulder seems to be localized at a molecular weight about two times higher than the molecular weight of the main peak. We have tried to rebuild the complete MWD of this

sample from the MWD of its cleaved arms[13]. In order to do this, we add up three different MWDs: a peak at 6 times the molecular weight of the cleaved arms represents the molecular weight of the corresponding 6-arm stars; a peak at 12 times the molecular weight of the arms represents coupled "pom-pom molecules"; and the last distribution is equal to the one of the cleaved arms (for residual linear chains). A last square minimization procedure has been used to calculate the proportion of each distribution (see Figure 6.b.). In this way, we have found that the best approximation of the complete MWD is composed of 81% of 6-arm star molecules, 2% of linear chains and 17% of pom-pom molecules.

5.4. CONCLUSIONS

In this work we have studied the LVE behaviour of linear and, for the first time, of polydisperse 6-arm star predominantly syndiotactic PMMA samples. We have found that the frequency-temperature superposition principle is fulfilled by both, linear and branched species, and that the shift factors follow the WLF equation. No sign of thermorheologically complex behavior is observed for star PMMA polymers. The entanglement state defined by G_N^0 is similar to the one observed for linear samples of similar tacticity. The Rouse relaxation time has been derived from chemistry independent variables by plotting $\eta_0 G_N^0/\tau_e$ *versus* N_e. The experimental linear viscoelastic response of the samples has been compared with predictions using our new model, which is able to account for the effect of the molecular weight distribution of the arms. In general a very good agreement between the predictions and the experimental results has been observed, with the same set of material parameters used for both linear and star samples,. This good agreement between experiments and theory also confirms the precision of the techniques used to synthesize and characterize the star PMMA analyzed in this work[13]. Nevertheless, for one of the star samples (S500), disagreement between rheological predictions and experiments, together with the

observation of a shoulder on its MWD, seems indicate the presence of some star-star coupling molecules.

REFERENCES

1. de Gennes, P.G., Scaling Concept in Polymer Physics (Cornell University Press, Ithaca, New York, 1979)
2. Doi, M. and S.F. Edwards, The Theory of Polymer Dynamics (Clarendon, Oxford, 1986)
3. C. Pattamaprom, R.G. Larson, T.J. Van Dyke. Quantitative predictions of linear viscoelastic rheological properties of entangled polymers. *Rheol. Acta*, 39: 517-531, 2000.
4. R.G. Larson, T. Sridhar, L.G. Leal, G.H. McKinley, A.E. Likhtman, T.C.B. McLeish*, J. Rheol*., 47, 809-818, 2003.
5. S.T. Milner, T.C.B. McLeish, *Macromolecules*, 30: 2159-2166, 1997.
6. G. Marrucci. *J. Polym. Sci., Polym. Phys.*, 23:159-177, 1985.
7. R.C. Ball, T.C.B. McLeish, 29:5717-5722, 1989.
8. C.H. Adams, L.R. Hutchings, P.G. Klein, T.C.B. McLeish, R.W. Richards, *Macromolecules*, 29 (17):2717-5722, 1996.
9. T.C.B. McLeish, S.T. Milner. Entangled dynamics and melt flow of branched polymers. *Adv. Polym. Sci.,* 143:195-256, 1999.
10. B. Blottière, T.C.B. McLeish, A. Hakiki, R.N. Young, S.T. Milner, *Macromolecules*, 31:9295-9304, 1998.
11. A.L. Frischnecht, S.T. Milner, A. Pryke, R.N. Young, R. Hawkins, T.C.B. McLeish, *Macromolecules*, 35:4801-4820, 2002.
12. E. van Ruymbeke, R. Keunings, C. Bailly, accepted in J. N. N. F. M., 2005.
13. L. Xue, U.S. Agarwal, M. Zhang, B.B.P. Stall, A.H.E. Müller, C. Bailly, P.J. Lemstra, "Synthesis and direct Topology Visualisation of High Molecular Weight Star PMMA", accepted in Macromolecules, 2005.
14. J.F. Vega, L. Xue, U. S. Agarwal, E. van Ruymbeke, R. Keunings, C. Bailly, "Linear rheology of polydisperse linear and star-shaped poly-(methyl methacrylate)", in preparation, 2005.

15. L. Xue, U.S. Agarwal, P.J. Lemstra, Macromolecules, 35, 8650, 2002.
16. Ferry, J.D. Viscoelastic Properties of Polymers, 3rd ed. (John Wiley and Sons. New York, 1980)
17. Porter, R.S., Know, J.P., Johnson, J.F. Trans. Soc. Rheol, 12, 409, 1968.
18. Carella, J.M., Grotto, J.T., Graessley, W.W. Macromolecules, 19, 659, 1986.
19. Bero C.A. and Roland C.M. Macromolecules, 29, 1562, 1996.
20. Wu, S. J. Polym. Sci.: Polym. Phys. Ed., 27, 723, 1989.
21. Fuchs, K.; Friedrich, Chr.; Weese, J. ;Macromolecules, 29, 5893, 1996.
22. Wu, S. and Beckerbauer, B., Polym. J., 24, 1437, 1992
23. Graessley, W. W.; Roovers, J. Macromolecules, 12, 959, 1979.
24. Roovers, J. Polymer, 26, 1091, 1985.
25. Rochefort, W.E.; Smith, G.G.; Rachapudy, H.; Raju, V.; Graessley, W.W. J. Polym. Sci.: Polym. Phys. Ed., 17, 1197, 1979.
26. Santangelo, P. G.; Roland, C. M.; Puskas, J. E. Macromolecules, 32, 1972, 1999. PIB
27. Fetters, L.J.; Graessley, W.W.; Kiss, D. Macromolecules, 24, 3136, 1991.
28. Fetters, L.J.; Lohse, D.J.; Witten, T.A., and Zirkel, A. Macromolecules;, 27, 4639, 1994.
29. Fetters, L.J.; Lohse, D.J.; Graessley, W.W. Macromolecules, 37, 1023, 1999.
30. S.T. Milner, T.C.B. McLeish, R.N. Young, A. Hakiki, J.M. Johnson. Macromolecules, 31, 9345-9353, 1998.
31. S.J. Park, R.G. Larson, J. Rheol., 47:199-211, 2003.
32. R.H. Colby, M. Rubinstein. Macromolecules, 23, 2753-2757, 1990.
33. Raju, V. R.; Menezes, E. V.; Malkin, G.; Graessley, W. W.; Fetters, L. J. Macromolecules, 14, 1668, 1981.
34. M.J. Struglinski, W.W. Graessley. Macromolecules, 18, 2630-2643, 1985.
35. S.J. Park, R.G. Larson. J. Rheol., 47, 199-211, 2003.
36. Tsenoglou C., Macromolecules, 24, 1762, 1991
37. des Cloizeaux, J., Europhys. Lett., 5, 437, 1988.

38. F.R. Schwarzl, , Rheol. Acta, 10, 166-173, 1971.